Scanning Microscopy

Volume 2 | Number 1 Article 8

9-15-1987

Applications of Transmission Electron Microscopy to Coal

C. A. Wert
University of Illinois

K. C. Hsieh
University of Illinois

Mike Buckentin
University of Illinois

B. H. Tseng
University of Illinois

Scanning Microscopy, Vol. 2, No. 1, 1988 (Pages 83-96)
Scanning Microscopy International, Chicago (AMF O'Hare), IL 60666 USA

0891-7035/88$3.00+.00

APPLICATIONS OF TRANSMISSION ELECTRON MICROSCOPY TO COAL

*C. A. Wert, K. C. Hsieh, Mike Buckentin and B. H. Tseng

Materials Research Laboratory
and Department of Materials Science and Engineering
University of Illinois
Urbana, IL 61801

(Received for publication June 22, 1987, and in revised form September 15, 1987)

Abstract

Coal consists of a hydrocarbon matrix in which minerals are embedded. The hydrocarbon matter also contains impurities distributed as individual atoms. Thus, coal has phases similar to those in metallic or ceramic alloy systems; a matrix, included precipitates and atoms distributed individually in solid solution. Consequently, techniques of electron microscopy developed to examine metallic and ceramic alloy systems are directly applicable to coal. We report application of microanalytical techniques of electron microscopy to coal using examples of measurements for several coals. Identification and characterization of clays and sulfides is described. Use of x-ray emission spectroscopy for organic element measurement is emphasized.

Key words: Coal, Minerals, Organic Sulfur, Transmission Electron Microscopy, Clays, Electron Diffraction, Pyrite, Maceral, Chlorine, Energy Loss Spectroscopy.

Address for correspondence:
*C. A. Wert
Department of Materials Science and Engineering
University of Illinois at Urbana-Champaign
1304 W. Green Street
Urbana, Illinois 61801
Phone No. (217) 244-0998

Introduction

Solid fuels such as coal and oil shale are composed of a hydrocarbon matrix with a great variety of embedded minerals. The principal minerals are clays (aluminum silicates), sulfides and oxides; in coal they may constitute up to 1/3 of the mass. Identification of the minerals, determination of their concentration and distribution and analysis of the changes they undergo when coal is heated or treated chemically can be carried out effectively using the techniques of electron microscopy.

The hydrocarbon material itself is not a uniform phase. Variations in chemical composition exist because of variations in the plant materials from which coals are derived and because of differences in the process of coalification. These differences can be examined by chemical analysis, but also by optical reflectance, by polarized light, by uv fluorescence, and by many other spectroscopic methods. Such investigations are crucial to an understanding of how the hydrocarbon matter is chemically fragmented during combustion, gasification or liquefaction.

The hydrocarbon matrix contains many heteroatoms, among them sulfur, chlorine and metallic elements. Chemical methods have been developed by coal scientists and geologists for determining the concentration of these organic elements. Electron optical methods are valuable adjuncts to these earlier techniques, as will be described.

This paper has the goal of describing transmission electron microscope (TEM) applications to the analysis of the hydrocarbon matrix, the associated minerals and the organically-bound elements. We give examples of both the diffraction techniques and microchemical analytical techniques included in the repertoire of TEM methods. Specimen preparation, both of thin coal films and fine coal powders, is not described; it is reported in several publications (24,25,32,33,55).

The Hydrocarbon Matter

Coal consists of a great variety of hydrocarbon phases derived from a myriad of plant materials, such as cellulose, lignin, spores, waxes, cutins, algae, partially oxidized

wood and many others. Since these materials vary in hydrocarbon composition, the resultant phases in the coals also vary in composition. Three main groups are identified: vitrinite, derived from woody tissue; exinites, derived from spores, cutins, waxes, and algae; and inertinite, derived from partially oxidized wood and other residues. Identification and characterization of these maceral types have been reviewed previously by Van Krevelen and by Winans and Crelling, among many others (53,59).

Two aspects of TEM aid in elucidation of coal structure. First, the general bright field images show some variation among these several maceral types (11). An optical micrograph of a sporinite maceral (one of the exinites) embedded in a vitrinite maceral is shown in Fig. 1a. Both macerals are featureless, even though the sporinite maceral is darker in this print than is true of the vitrinite. The many black and light spots in the vitrinite are minerals. When two adjacent macerals are thinned for transmission electron microscopy and examined in a bright field image, one sees the images in Fig. 1b. The vitrinite and sporinite macerals have quite a different appearance. The sporinite has an irregular twisted structure with highly variable electron density, apparently because of a variable spatial structure of the flattened spherical spores. The vitrinite is a more homogeneous material, apparently because of a linear cell structure of the original wood. An example of a fusinite structure (one of the inertinites) is shown in Fig. 2. An optical micrograph of a thinned specimen prepared for electron microscopy is shown in 2a, where one can see the outlines of the original wood cells. The dark spot in the center is a perforation. The electron micrograph image of a feather edge next to this perforation, Fig. 2b, shows again a featureless structure at this high magnification. Use of transmission electron microscopy to characterize the structure of macerals has been reported earlier by Harris and his colleagues and by

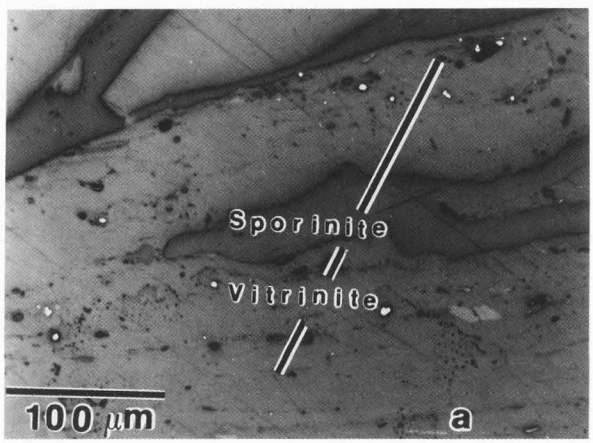

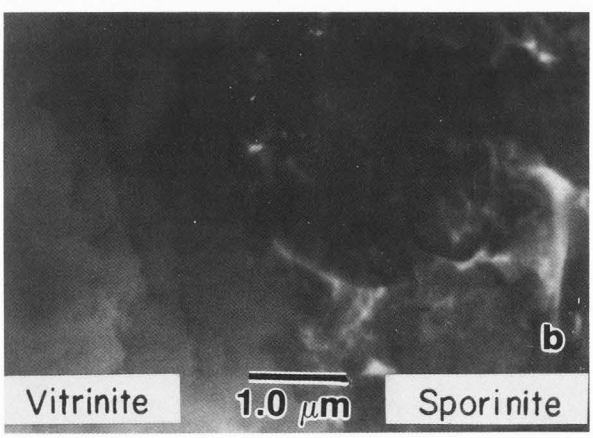

Fig. 1. a. Optical image of a vitrinite maceral containing an embedded sporinite maceral.
b. Bright field TEM image of adjacent sporinite and vitrinite macerals.

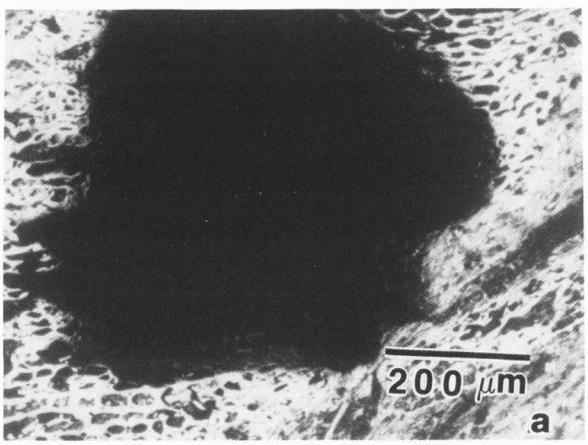

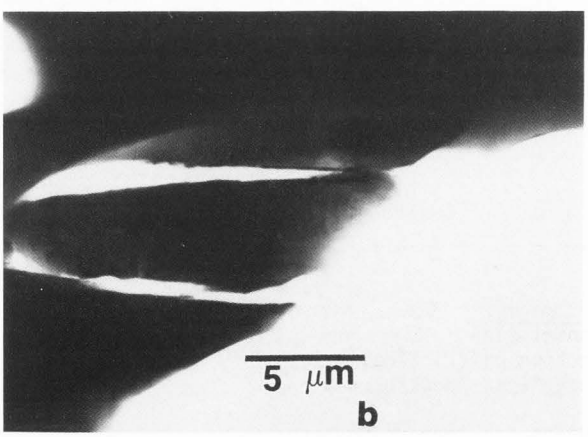

Fig. 2. Optical (a) and bright field (b) TEM image of an inertinite maceral.

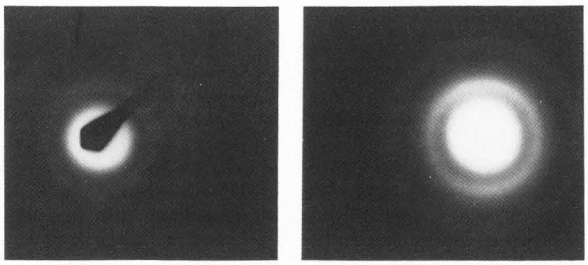

Fig. 3. Amorphous rings of electron diffraction patterns of Illinois coals #5 (left) and #6 (right).

McCartney (26,36). Their photographs are similar to those shown here. All of these micrographs give some information, but it is not an outstanding application of transmission electron microscopy.

Coal is usually considered to be an amorphous solid. To test that hypothesis, we have made many diffraction studies of thin coal films. A typical example is shown in Fig. 3. Only rings characteristic of amorphous material can be seen. We have never seen structure on these rings or individual spots for any coal specimens. Films of amber, a phase analogous to resinite in coal, also show only diffuse rings, again characteristic of an amorphous structure. Attempts to determine a microtexture in coal using electron diffraction techniques are reported by Rouzaud and Oberlin (42); the basic structural units reported for 60 coals of all ranks are described as being less than 1 nm in size. Electron microscopy of certain synthetic polymers shows lamellae much larger than this (17).

Minerals in Coal

Coal contains many types of minerals. Furthermore they are often times present in large quantity -- up to 25% or more in some coals. The origin of these minerals is diverse. Some formed in peat bogs and swamps. Others entered the coal through dust particles, wind blown or of volcanic or meteoric origin. X-ray diffraction techniques allow identification of many types of minerals in coal; the scanning electron microscope shows the presence of many additional minerals (16,19,20). Transmission microscopy shows even additional minerals (1,2,27,45). Both the SEM and TEM techniques permit imaging of individual particles of minerals not plentiful enough to provide coherent x-ray diffraction patterns. In this section, we focus on two mineral-types, the clays and sulfides.

Clay

The clays are important because they are present in such large quantity that they produce a great deal of ash when coal is burned. One of the common clays kaolinite, $Al_2Si_2O_5(OH)_4$, can be identified positively by use of its diffraction pattern combined with its x-ray emission spectrum (EDS).

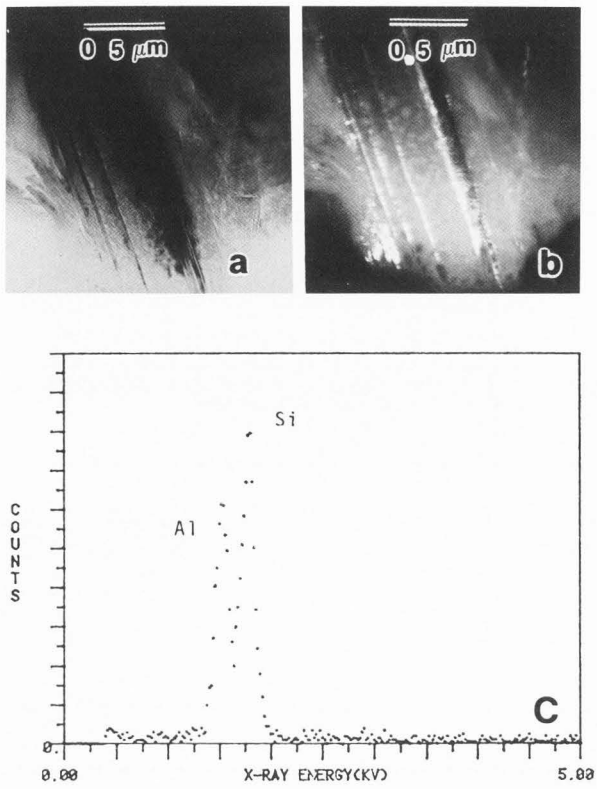

Fig. 4. A kaolinite clay. a. Bright field image of a lamellar structure. b. Dark field image of the lamellae. c. EDS pattern shows lines of Al and Si.

A typical kaolinite structure is shown in Fig. 4. The bright field image, 4a, shows a lamellar pattern; the dark field image, 4b, shows that the lamellae are nearly single crystals. Its EDS pattern, 4c, shows lines only of aluminum and silicon, the composition of kaolinite. Finally electron diffraction identifies the kaolinite structure. A detailed description of the clays, both of kaolinite and of other more complex clays, is given in the book by Brindley and Brown (6).

Not all kaolinites have this lamellar structure. Because of disorder in layering sequences, some clays are found in tubular form, one type of which is called halloysite. Such a clay is present in a Western coal from Routt county, near Steamboat Springs, Colorado. Bright field images of this clay are shown in Fig. 5. X-ray diffraction and EDS measurements show this to be a kaolinite, but clearly a stacking mismatch has caused the plates to curl into a rounded form. Details of the halloysite structure are found in pages 146 to 161 of reference 6.

Numerous applications of TEM to the structure of clays have been reported earlier (14,21,29,31,37,40,52,54,58). Some of these are superb applications of microscope techniques: bright field, dark field, electron diffraction, high resolution, EDS, etc. Of particular interest to this paper are the observations of

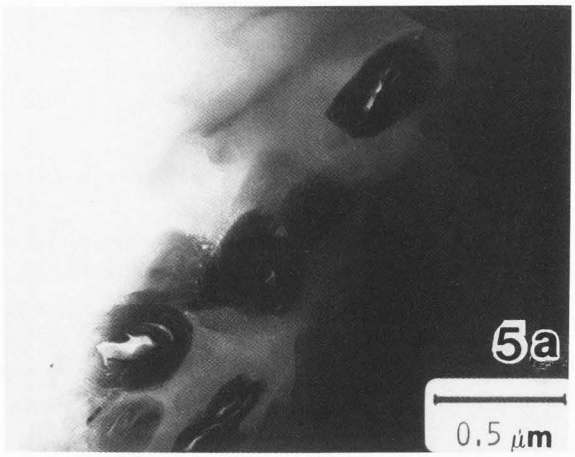

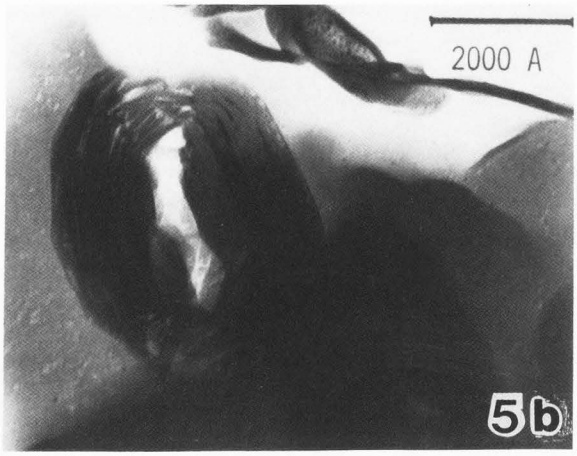

Fig. 5. The folded structure of kaolinite in a halloysite-like structure at two levels of magnification.

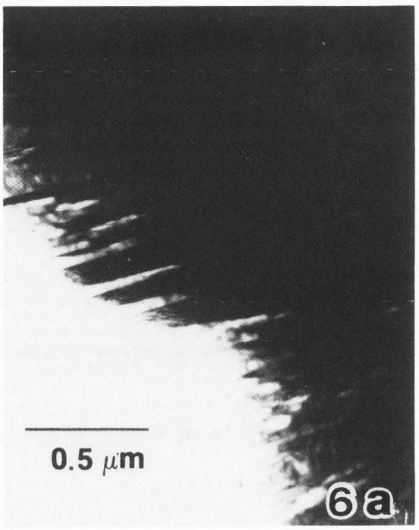

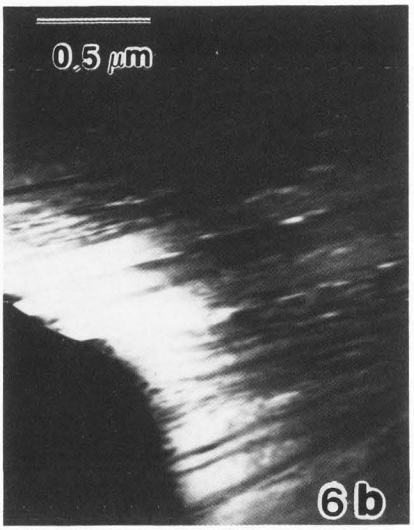

Sudo and his colleagues on the mineral halloysite (46,47). They show many photomicrographs of tubular halloysite and of spherulitic halloysite similar in appearance to that of Fig. 5. See plates 16-21 of reference 47.

Other metal ions may substitute for some of the aluminum and silicon, which together with changes in structure form clays called illites. The variety of substitutions which can take place is enormous; a few examples are given on page 78 of reference 2. A particular illite in a bituminous sample of Illinois #5 is shown in Fig. 6. This is a potassium substituted clay. Its bright field and dark field images show a typical lamellar pattern with large single crystal lamellae. The EDS spectrum shows the presence of potassium.

One of the features of electron diffraction not much used by mineralogists is that of dark-field-image-formation. That type of image, shown for kaolinite in Fig. 4 and illite in Fig. 6, is obtained using the electron beam diffracted at a specific angle off a specific set of planes of a crystalline specimen. If the

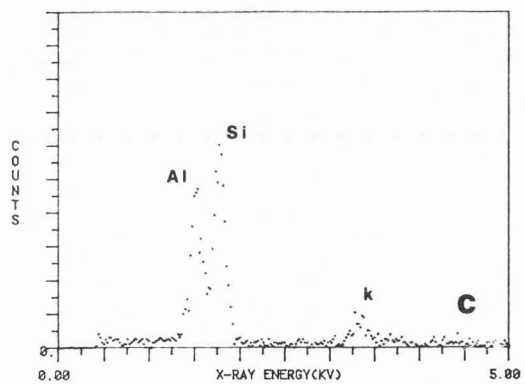

Fig. 6. Bright field, a, and dark field, b, images of an illite. The EDS pattern, c, shows the presence of K as well as Al and Si. The single crystal lamellar structure is evident.

image is uniformly illuminated, the specimen is a single crystal. The dark-field-images of Figs. 4 and 6 show that not only are the individual clay lamellae single crystals, but

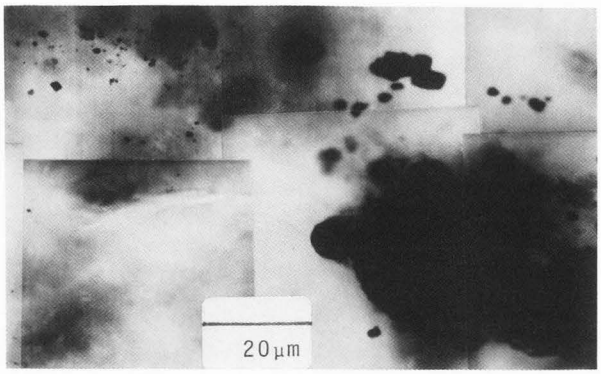

Fig. 7. General panoramic map of mineral distribution in coal.

also that all lamellae have about the same spatial orientation -- the clay particle is like a single crystal.

Not all clays have these lamellar or tubular forms. Many of them are mixed and twisted masses, often associated with other minerals. These are described in a number of publications, in particular by Renton (41).

Sulfide Minerals

The sulfur compounds are troublesome minerals in coal, since the sulfur usually goes off as a sulfur-oxide or as H_2S upon combustion or chemical treatment. Electron microscopy offers two significant avenues of study: identification of the forms of sulfur present in coal and determination of changes which take place when the sulfides are oxidized or reduced.

The most important sulfides are the disulfide FeS_2 and the monosulfide Fe_xS. The first of these is ideally stoichiometric, the second is always iron deficient, with x varying between 0.85 and 1.0. Crystallographic parameters and the chemistry of these sulfides are discussed in earlier publications. Pyrite was one of the first crystals whose structure was determined by x-rays. Measurements for pyrite, marcasite and the pyrrhotites may be found in the following references (5,8,9,12,13,30,31,34).

Transmission electron microscopy permits identification of several additional features of the sulfides. First, low magnification images permit the mapping of the mineral distribution over a relatively large volume. Such a picture for an Illinois #5 coal is shown in Fig. 7. This figure was made using the scanning mode of the Vacuum Generators HB 5. By altering the amplifier gain of the instrument, the montage photograph of Fig. 7 could be made from the thinnest sections into thicker sections of the wedge, a procedure not easily carried out without the scanning capability. This type of measurement supplements information that can be learned using an SEM, but like the SEM, it does not differentiate among the mineral types.

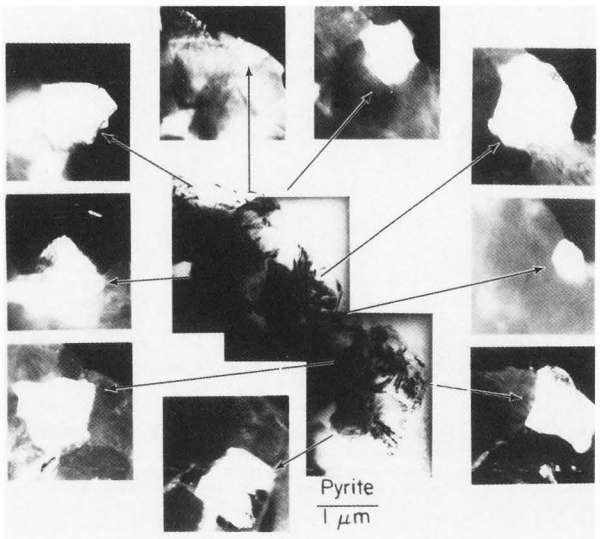

Fig. 8. A polycrystalline pyrite.

Examination of the individual particles permits easy identification of the sulfides. First, polycrystalline pyrite is easy to identify. The bright field image of a polycrystalline pyrite particle shows its overall shape, see Fig. 8. Tilting the specimen into the proper diffraction angle for each of the single crystals making up this massive polycrystal permits identification of the single crystal units. The individual crystallites about the perimeter of this figure are imaged one-by-one in dark field illumination.

The single crystal character of certain particles is also easy to see using dark field illumination. Figure 9 shows one such mineral. Clearly this particle, of size a few μm, is a single crystal. The EDS spectrum, together with the diffraction pattern, identify it as pyrite.

A third form of sulfide aggregation are the framboids. These are small single crystals of pyrite which have formed in a compact spherical mass, Fig. 10. They always have the composition of the disulfide and the individual crystallites appear to have no crystallographic relationship to the others within the mass.

A final example of an electron diffraction technique applicable to minerals is convergent-beam-diffraction (7). In this technique, the incident electron beam is not a parallel beam, but impinges on the specimen in a small cone of convergence, about 1°. Diffraction spots are both spread into a disk and are not uniformly illuminated; each has a variable intensity which depends on the symmetry of the specimen crystal (7). Further, in a particular mode, a pattern such as that shown in Fig. 11 is produced. This High-Order-Laue-Zone (HOLZ) pattern permits determination to be made of interplane spacing to an accuracy about an order-of-magnitude

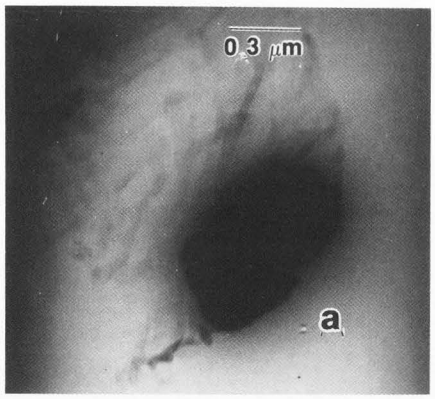

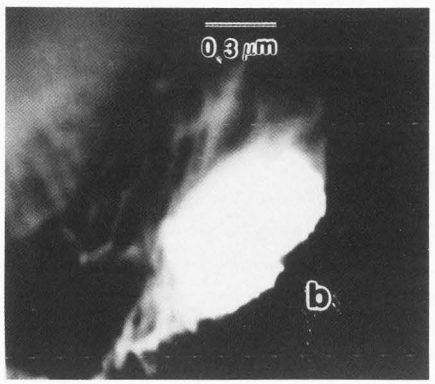

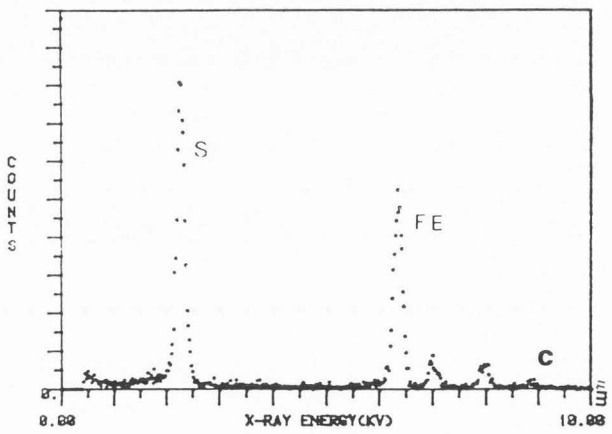

Fig. 9. Analysis of a single crystal of pyrite. a. Bright field. b. Dark field. c. EDS spectrum.

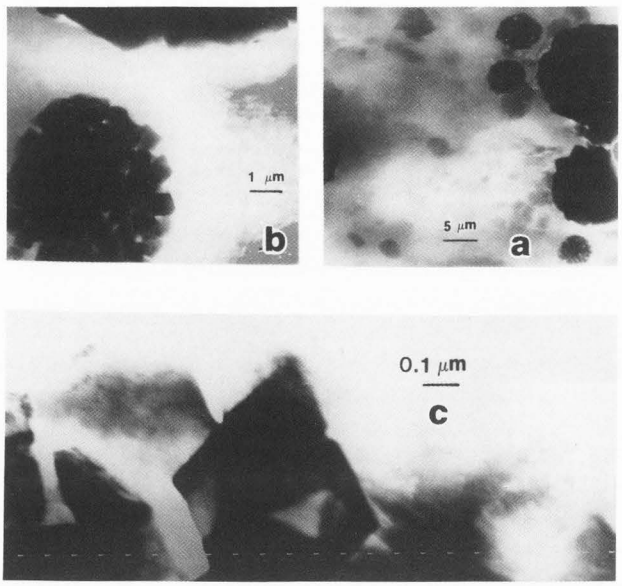

Fig. 10. A framboidal pyrite cluster at 3 levels of magnification.

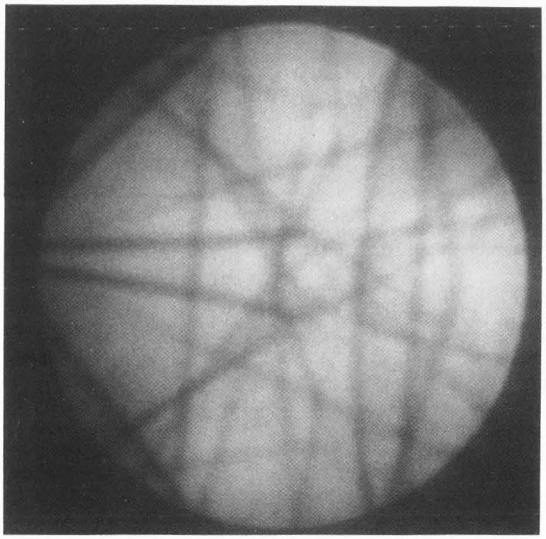

Fig. 11. Convergent beam analysis of a pyrite crystal.

higher than use of selected-area-diffraction methods. For this single measurement, calculations from the lines in Fig. 11 permit the cube edge of pyrite to be determined as 5.42 Angstroms, compared to the accepted value of 5.417 Angstroms.

The disulfide may also exist as an orthorhombic structure, marcasite. Using such diffraction patterns the cell dimension a = 3.35Å, b = 4.40Å and c = 5.35Å were easily obtained, again in good agreement with published values.

Finally, Y. P. Ge and K. C. Hsieh have measured in our laboratory the exact structure and cell size of oxides produced from oxidation of pyrite after coal is heated into the range

400°C to 600°C (51). That work utilized both selected area diffraction and convergent beam diffraction.

Identification of the composition and structure of the monosulfide, pyrrhotite, is a more formidable task. First, the chemistry is not ideally stoichiometric, since the iron sublattice contains vacancies, up to 15%. Furthermore, these vacancies may be ordered, so that a superlattice structure may exist. Two particular composition ranges are important. First, a monoclinic compound has composition Fe_7S_8. This structure is, in fact, nearly hexagonal since the monoclinic angle is within 1° of being a right angle. Second, composition ranges between $Fe_{0.9}S$ and FeS yield a hexagonal pyrrhotite, but the iron ion vacancies are ordered into stacking patterns not only of the ideal hexagonal symmetry 2C, but also of polytypes of symmetry 3C, 4C, etc.

Pyrrhotite in coal and coal products has not been studied extensively. However, a large literature exists on the structure of mineral pyrrhotite, mostly on the hexagonal form (30,31). These papers allow interpretation of measurements on pyrrhotite in coal in terms of structure and composition with high accuracy, as we note in the next section.

Decomposition of Pyrite

Pyrite undergoes a peritectic phase transformation at 740°C in equilibrium with sulfur vapor and the monosulfide. In the presence of oxygen, the transformation proceeds at a somewhat lower temperature; it is found that pyrite begins to decompose at about 400°C (48). The first product is pyrrhotite, which further oxidizes to an oxide of iron in the presence of sufficient oxygen. The first step of this reaction, alteration of a small single crystal of mineral pyrite, was followed by Tseng using SEM and electron diffraction. The succession of events is shown in Fig. 12. The crystal was a small sedimentary cube about 2 mm on a side Fig. 12a. After a few minutes at 470°C in a vacuum, surface nuclei of pyrrhotite formed, Fig. 12b. Gradually nuclei grew and impinged, the surface of the crystal after 30 minutes appeared as in Fig. 12c. A cross section of the crystal at that point shows a columnar growth of pyrrhotite on the decomposing pyrite, Fig. 12d. The interface between the two is a plane. This interface moves uniformly into the pyrite with time. This seems to be true because the fibrous growth of pyrrhotite is constrained by the underlying pyrite, so that the reduction of volume which occurs in the transformation permits fresh interface always to be exposed to the atmosphere. Tseng's measurements at temperatures between 470 and 525°C in vacuum yielded an activation energy near 30 kcal/mole; in dry nitrogen about 64 kcal/mole. Other investigators who previously have measured the kinetics of this phenomenon also find variable activation energies between 30 and 60 kcal/mole.

Measurements by x-rays of the d(102) spacing of this initial pyrrhotite show that it

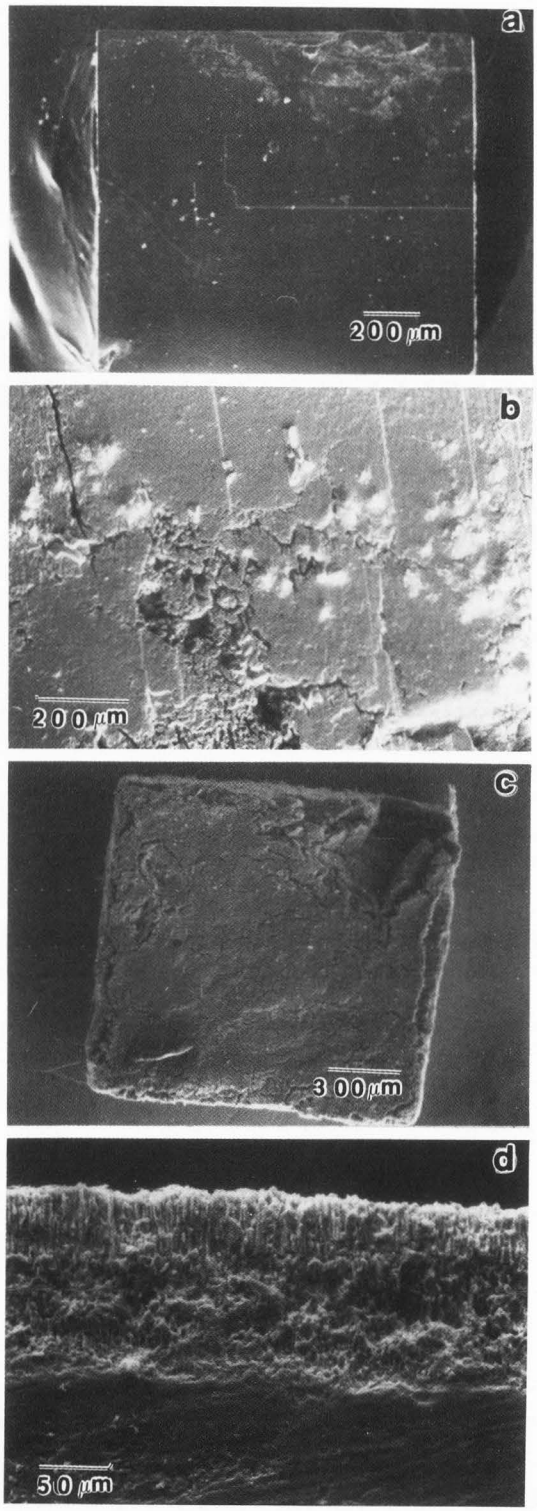

Fig. 12. Decomposition of pyrite to pyrrhotite. a. Initial pyrite crystal. b. Pyrrhotite nuclei on surface. c. Columnar pyrrhotite. d. Cross section of pyrite-pyrrhotite aggregation.

has a relatively low initial composition of iron, near $Fe_{0.9}S$ and is probably hexagonal. Upon prolonged treatment the Fe/S ratio increases and finally approaches FeS. For these calculations, Tseng used the data of Arnold and Reichen for d(102) spacing as a function of composition (3,4). All of these pyrrhotites contain an ordered array of iron vacancies; the structure changes with time, finally approaching the 2C structure characteristic of troilite FeS.

Unpublished data of Tseng and Hsieh from heating experiments on coal indicate that pyrite crystals embedded in coal have similar modes of decomposition.

Organic Impurities

Most impurities in coal exist as minerals. However, some impurities are distributed atom-by-atom through the hydrocarbon material, replacing C or O atoms in either the aromatic or the aliphatic constituent. In addition, some impurities are attached as side appendages on the aromatic rings. The concentration of these distributed heteroatoms may be measured by many of the same techniques used for solid solutions in metallic and ceramic alloys.

Consider sulfur as an important example. The standard ASTM technique for determination of organic sulfur is a three step process. First the total sulfur is determined chemically. Then by selective dissolution of the sulfides and sulfates, the sulfur concentration of these two compounds is determined. The organic sulfur is defined as the difference between the total sulfur and that measured for the compounds. The first attempt to apply electron optical methods for direct measurement of organic S used SEM techniques. The sulfur concentration was determined from the count rate of the sulfur Kα count rate after appropriate calibration using standard sulfur compounds (38,39,44).

This technique has proved to be valuable. It permits determination of the sulfur concentration by a direct means and the measurement is made on a relatively small volume of about 100 μm^3. In practice, correction for the presence of pyrite and sulfate must be made because a reasonable chance exists that a mineral compound of sulfur may exist in the volume of measurement. However, the presence of minerals can be ascertained if the Kα line of iron is present. Appropriate correction procedures have been developed to take account of that possibility.

The transmission electron microscope also can be used for measurement of organic impurities. The Kα or Lα lines might be used to determine the presence of organically-bound elements. Furthermore, the thin specimen gives much smaller beam spreading than is true for the SEM (or the electron microprobe), so the volume of measurement is much smaller, less than 1 μm^3. Furthermore, minerals are easily seen in the bright field image, so the point of measurement may be placed in a clear field. Thus the x-ray signal can be assigned to the organic constituent with confidence. The remaining problem is measurement of the thickness of the foil.

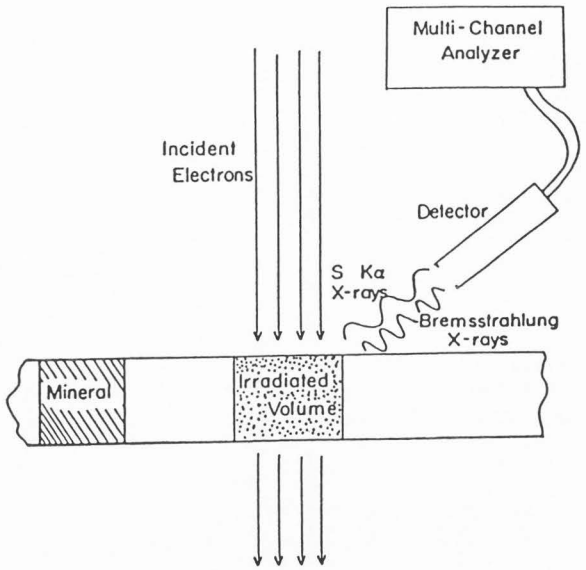

Fig. 13. TEM assembly for measurement of organic elements in coal.

The geometry of the specimen and detector is shown in Fig. 13. The Kα x-ray line is counted with an energy-dispersive detector. The thickness of the foil is determined utilizing the Bremsstrahlung radiation is counted simultaneously with the Kα line of the organic element being measured. The concentration of the organic impurity, in our case sulfur, is given by the linear equation

$$\text{wt. \% S} = A\, C_s/C_b$$

Here, the ratio of the count rates for sulfur, C_s, and the Bremsstrahlung, C_b, multipled by a calibration constant, A, gives the weight percent of the organic element. Details of the origin of this expression can be found in papers of Hall (22,23) and of Shuman, Somlyo and Somlyo (43).

Several conditions are necessary for successful application of this method. The electron beam should not be appreciably attenuated by the foil. A thin foil thus assures that the production of x-rays is not a function of depth in the foil. Second, fluorescence and absorption must be absent; this criterion has been discussed by Goldstein and others (18); for coal and similar hydrocarbon substances a thickness less than 500 nm is satisfactory. Thirdly, the constant A should be approximately a constant for all coals, even with variations in the hydrocarbon composition. Since the Bremsstrahlung radiation comes principally from the carbon and oxygen atoms, and since the contribution is approximately proportional to the atomic number squared, some variation is expected depending on the rank of the coal. However, we calculate

that A should not vary more than 5% in going from lignite to anthracite. Most of our measurements have been on the bituminous coals, for which the constant A varies even less with rank.

Tseng and Hsieh determined the constant A using three sulfur forms, pure sulfur, a thiophene and a sulfone (28,48). The constant initially had the value of 1.6; subsequent changes in the detector have resulted in small changes. Shift of the counting efficiency of the detector and consequent change of A can easily be checked by periodic recalibration.

Three advantages accrue from the use of this thin film technique. First, it is a direct measurement and interferences from mineral sulfur can easily be avoided. Second, the volume of measurement is so small (typically less than 10^{-12} cc) that short range variations of sulfur concentration in coal may be easily measured. Third, the use of the Bremsstrahlung radiation avoids the necessity for separate measurements of the foil thickness, a determination fraught with error.

Types of Measurement

At least four types of measurement are possible using this technique: measurement of the average organic sulfur concentration, determination of spatial variation of sulfur content, measurement of variation of organic sulfur by maceral type and the monitoring of changes in organic sulfur during heating of coal. In addition, concentrations of other organic elements can be measured after appropriate calibration.

Measurement of the average organic sulfur content of coal requires that a number of individual measurements on separate volumes be determined so that the average gives a reliable number for that coal. The requirement of multiple measurements comes not from an inherent difficulty with the technique; rather it arises because the organic sulfur concentration in coal varies from place to place and from maceral type to maceral type. We have investigated the number of measurements which must be made to get a good average. For most coals, the average converges to a constant value after about 25 measurements on random fine powders. For a few coals in which the organic sulfur content has wide variation from powder particle to powder particle (Illinois #6, for example), the average converges more slowly, so we typically use 50 or more individual measurements. For coal foils, a wide sampling of many areas must be made to assure that all maceral types are sampled in proportion to their fraction of the whole coal.

Measurements on 6 coals for which we have corresponding ASTM values are shown in Fig. 14. If the TEM values and the ASTM values agree, the points should lie on the 45 degree line of that figure. They do and thus the TEM method does give values comparable to the standard ASTM technique. Other such comparisons are described in additional publications from our laboratory (28,50,57).

The spatial variation of organic sulfur across a maceral is shown in Fig. 15. Two

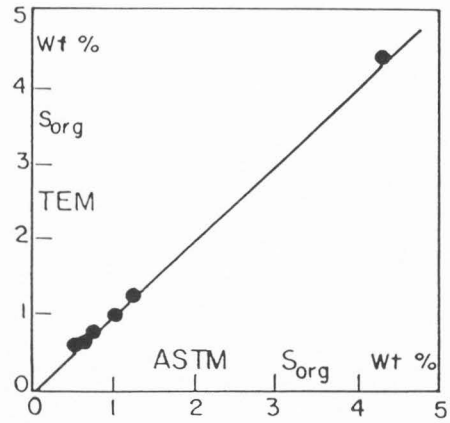

Fig. 14. Measurement of average sulfur concentration. Comparison of TEM and ASTM techniques.

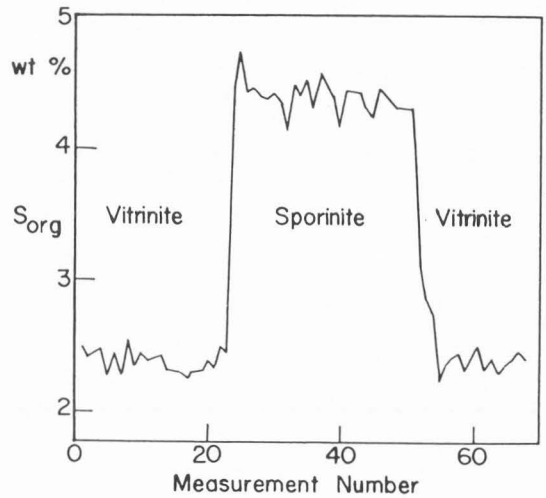

Fig. 15. Spatial variation of organic sulfur across a vitrinite and a sporinite maceral. These measurements were made along the dark line in Fig. 1a.

macerals are present here, a maceral of sporinite embedded in a large maceral of vitrinite. The variation from point to point in either maceral is about ±10% over this relatively short distance of a few hundred μm. However the variation between the maceral types is extremely marked, as the trace shows. The organic sulfur in the sporinite maceral is much higher than that in the associated vitrinite maceral. Furthermore the increase is abrupt at the boundary between the two maceral types.

The variation among these maceral types has been reported for four coals using macerals separated by centrifuge-gradient-techniques on finely pulverized coals (50). Those data and new measurements for an additional coal are presented in Fig. 16. For these five coals the variation of organic sulfur by maceral type

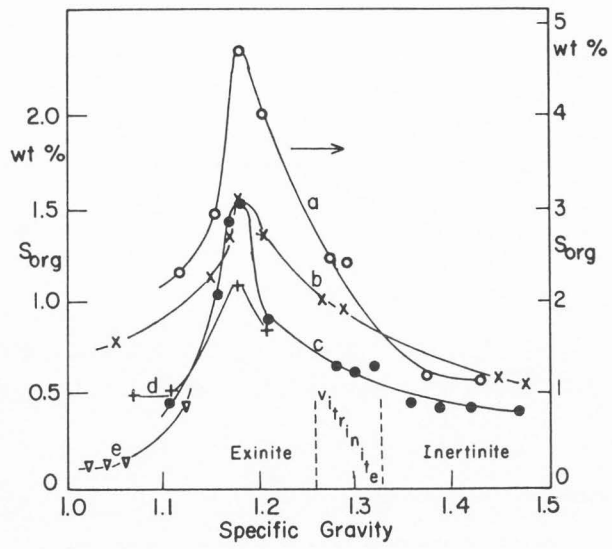

Fig. 16. Variation of organic sulfur by maceral type for 5 bituminous coals. These coals are the following: a. Illinois #5, b. Ohio #5, c. Indiana Block Coal, d. SIU 647J and e. Utah Cannel Coal.

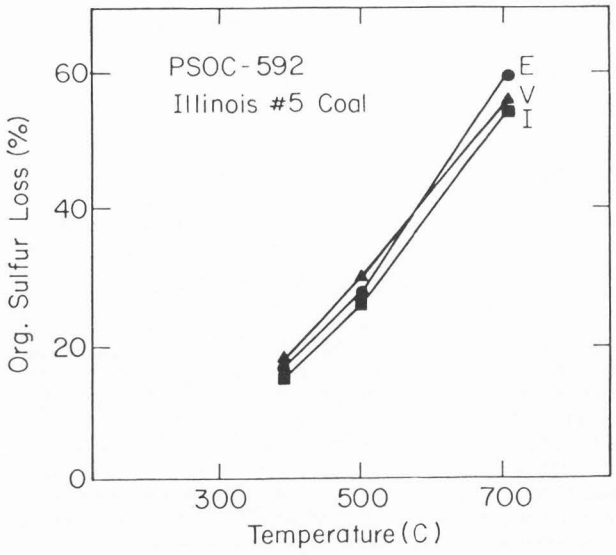

Fig. 17. Change in organic sulfur during heating of separated macerals.

follows a characteristic pattern, peaking at sporinite. Interestingly, the average organic sulfur content of these coals is nearly that of the vitrinites, as Raymond has pointed out for a number of coals earlier (38).

Finally, the change in organic sulfur content of macerals which have been heated has been measured for several coals (51). One example is shown in Fig. 17. For this and other coals, loss of sulfur occurs over the temperature range 400°C to 700°C. Furthermore, the macerals lose organic sulfur (fractionally) at the same rate.

Other Organic Elements

Chlorine is also distributed in coal atom by atom as well as being present in salts. We have measured the organic chlorine content of several coals, and we have determined the chlorine distribution in bituminous matter in gold ores. Bituminous matter is frequently found in ores in which the gold is finely disseminated as micron-sized particles. The presence of the bituminous matter affects the efficiency of gold recovery from these carbonaceous ores and chlorine may be used to improve recovery efficiency. We have found that the chlorine desulfurizes the carbonaceous matter of its organic sulfur (49). An example of two hydrocarbon particles containing sulfur, one untreated and one treated with chlorine is shown in Fig. 18. The original material has organic sulfur but no chlorine. The organic sulfur in the treated bituminous material is greatly reduced but some chlorine is picked up by the bituminous particle.

Organic chlorine and organic sulfur can be determined independently at the same time in a

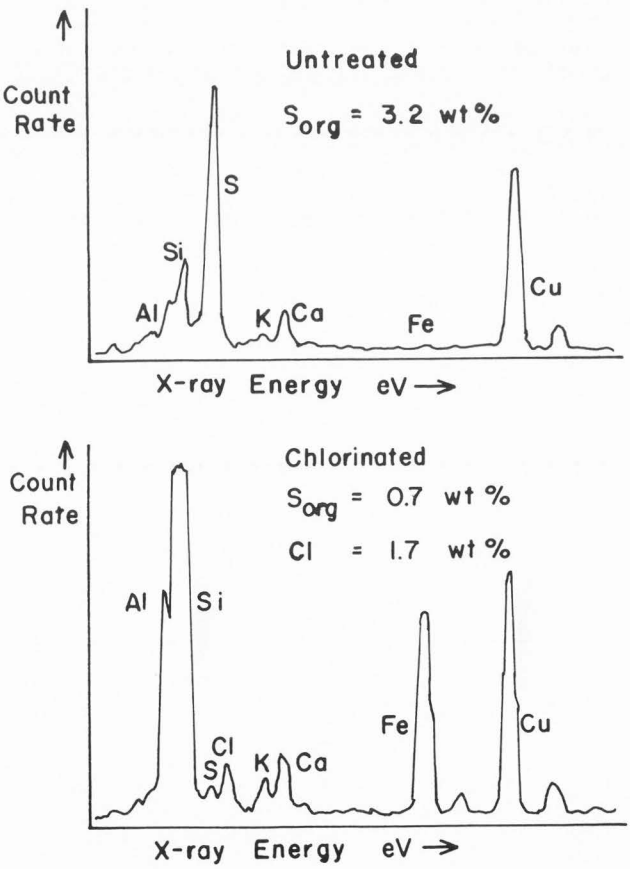

Fig. 18. Reduction of organic sulfur in bituminous matter treated by Cl at 40°C.

coal specimen since the Kα lines of the two elements are of sufficiently different wavelength. We have, in addition measured on the presence of "organic" iron. A Colchester #2 bituminous coal from Illinois showed the presence of the iron EDS line, even when no mineral precipitates were evident (57). This measurement is not fully conclusive since the sulfur line also coexisted with the iron line, so the presence of ultra-fine particles of iron-sulfide or of an oxide of iron cannot be ruled out.

Organic Oxygen

ASTM methods for determination of oxygen content are highly imprecise. The technique requires separate determinations of the total oxygen content of the coal and of the content bound up in clays and oxides (15,35). In principle the electron optical technique can resolve this problem, since the Kα line oxygen may be counted in a windowless detector. We have made a number of measurements, one of which is plotted in Fig. 19. One clearly sees that the x-ray lines of carbon and oxygen are separable and that the ratio of their areas has about the right value for such a bituminous coal. Making a more refined measurement of oxygen concentration or of the C/O ratio is not simple, however. The mass absorption coefficient of oxygen in coal is about three times that of carbon in coal, consequently, correction procedures are required to produce a reliable number. Criteria listed by Goldstein for correctionless measurement requires that a coal foil would need to less than 100 angstroms thick (18). Although thin edges of milled foils might be that thin, the measurement is still uncertain. Additionally, the deposition of carbon deposits on the surface of the measuring spot is difficult to prevent, so this measurement still needs refinement.

We have also reported application of Electron-Energy-Loss-Spectroscopy (EELS) in an attempt to measure the organic oxygen content of coal (56). That measurement showed the absorption edges of both carbon and oxygen, but again, quantitative analysis was not possible. However, successful application of EELS has been made many times for metallic alloys (10), and its success for coal seems likely with enough effort.

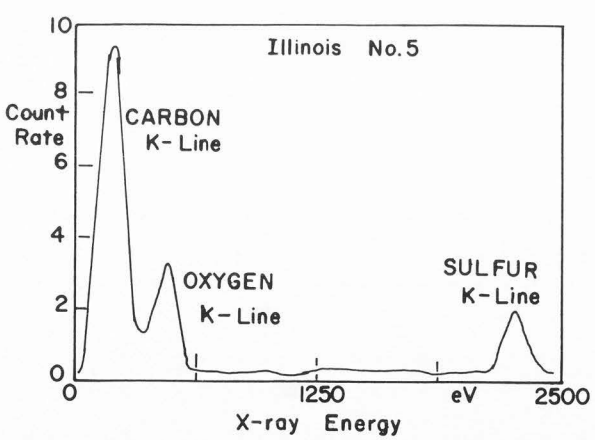

Fig. 19. EDS spectrum of carbon and oxygen from coal.

Summary

Microanalytical electron microscope techniques of Materials Science have important applications to coal structure and chemistry. Some details of the structure of the macerals may be made, as this and earlier measurements have shown. Identification of minerals and of changes in structure and composition upon heating is both reliable and rapid. This is not a good technique for measuring averages over mineral aggregations, though, since the particles are examined one-by-one. For organic constituents, though, the technique has great value, especially if spatial variation is an important consideration. Overall, transmission electron microscopy is a valuable tool for determination of the chemistry of coal.

Acknowledgements

Support for this work has been given by the Division of Materials Research, DOE, under contract DE-AC02-76ER01198.

References

1. Allen RM (1983) Microstructural Changes in Coal During Low Temperature Ashing, 1983 International Conference on Coal Science, 361-364, International Energy Agency.

2. Allen RM, VanderSande JB (1984) Analysis of Sub-micron Mineral Matter in Coal via Scanning Transmission Electron Microscopy, Fuel, 63, 24-29.

3. Arnold RG (1962) Equilibrium Relations Between Pyrrhotite and Pyrite from 325°C to 743°C, Econ. Geol., 57, 72-90.

4. Arnold RG, Reichen LE (1962) Measurement of the Metal Content of Naturally Occurring, Metal-Deficient, Hexagonal Pyrrhotite by an X-ray Spacing Method, Am. Mineralogist, 47, 105-111.

5. Barbier J, Hiraga K, Otero-Diaz LC, White TJ, Williams TB, Hyde BG (1985) Electron Microscope Studies of Some Inorganic and Mineral Oxide and Sulphide Systems, Ultramicroscopy, 18, 211-234.

6. Brindley GW, Braun, G (1980) Crystal Structures of Clay Minerals and Their X-ray Identification, Mineralogical Society, London.

7. Britton EG, Stobbs WM (1987) The Analysis and Applications of Dynamical Effects in HOLZ Patterns, Ultramicroscopy, 21, 1-12.

8. Brostigen G, Kjekshus A (1969) Redetermined Crystal Structure of FeS_2 (Pyrite), Acta Chem. Scand., 23, 2186-2188.

9. Brostigen G, Kjekshus A, Romming, C (1973) Compounds with the Marcasite Type Crystal Structure, Acta Chem. Scand., 27, 2791-2796.

10. Bruemmer SM, Fluhr CB, Beggs DV, Wert CA, Fraser HL (1980) An Analytical Microscopy Study of the High Temperature Carbide Formed in a V-5Ti-C Alloy, Met. Trans., 11A, 693-699.

11. Buckentin M (1985) Direct Determination of Organic Sulfur in Coal Macerals Using Transmission Electron Microscopy, MS Thesis, University of Illinois at Urbana-Champaign.

12. Buerger MJ (1931) The Crystal Structure of Marcasite, The American Mineralogist, 16, 361-395.

13. Couderc JJ, Bras J, Fagot M, Levade C (1980) Etude par Microscopie Electronique en Transmission de l'etat de Deformation de Pyrites de Differente Provenances, Bull. Miner., 103, 547-557.

14. Eberhart JB (1982) High Resolution Electron-Microscopy Applied to Clay Minerals, Developments in Sedimentology, 34, 31-50.

15. Ehmann WD, Koppenaal DW, Hamrin Jr CE, Jones WC, Tian WZ (1986) Comparison of Methods for the Determination of Organic Oxygen in Coals, Fuel, 65, 1513-1570.

16. Finkelman RB, Stanton RW (1978) Identification and Significance of Accessory Minerals from a Bituminuous Coal, Fuel, 57, 763-768.

17. Giorgio S, Kern R (1987) Defects in a Lamellar Polymer by High-Resolution Electron Microscopy, Ultramicroscopy, 21, 157-170.

18. Goldstein JI (1979) Principles of Thin Film X-ray Microanalysis, Introduction to Analytical Electron Microscopy, Hren JJ, Goldstein JI, Joy DC, Plenum Press, NY, 83-120.

19. Greer RT (1977) Coal Microstructure and Pyrite Distribution, ACS Symposium Series, 64, 3-15.

20. Greer RT (1978) Pyrite Distribution in Coal, Scanning Electron Microsc. 1978;I:621-627.

21. Guven N, Lafon GM, Lee LJ (1982) Experimental Hydrothermal Alteration of Albite to Clays: Preliminary Results, Developments in Sedimentology, 35, 495-511.

22. Hall TA, Anderson HC, Appleton T (1973) The Use of Thin Specimens for X-ray Microanalysis in Biology, Jour. of Microscopy, 99, part 2, 177-182.

23. Hall TA (1979) Biological X-ray Microanalysis, Jour. of Microscopy, 117, 146-163.

24. Harris LA, Yust CS, Crouse RS (1977) Direct Determination of Pyritic and Organic Sulfur by Combined Coal Petrography and Microprobe Analysis - A Feasibility Study, Fuel, 56, 456-457.

25. Harris LA, Braski DN, Yust CS (1977) A Study of Factors Affecting Elemental Analysis by STEM, Ceramic Microstructures, Ed. Fulrath, RM, Univ. California Press, Berkeley, 54-59.

26. Harris LA, Yust CS (1981) The Ultrafine Structure of Coal Determined by Electron Microscopy, Adv. Chem. Series, 192, 321-336.

27. Hsieh KC (1982) Transmission Electron Microscope Study of Mineral in Coal, Ph.D. Thesis, University of Illinois at Urbana-Champaign.

28. Hsieh KC, Wert CA (1985) Direct Measurement of Organic Sulfur in Coal, Fuel, 64, 255-262.

29. Inoue A, Kohyama N, Kitagawa R, Watanabe, T (1987) Chemical and Morphological Evidence for the Conversion of Smectite to Illite, Clays and Clay Minerals, 35, 111-120.

30. Koto K, Morimoto N, Gyoba A (1975) The Superstructure of the Intermediate Pyrrhotite. I. Partially Disordered Distribution of Metal Vacancy in the 6C Type, $Fe_{11}S_{12}$, Acta Cryst., B31, 2759-2764.

31. Koto K, Kitamura M (1981) The Superstructure of the Intermediate Pyrrhotite. II. One-dimensional Out-of-step Vector of Iron Vacancies in the Incommensurate Structure with Composition Range Fe_9S_{10} to $Fe_{11}S_{12}$, Acta Cryst., A37, 301-308.

32. Lauf RJ (1982) Microstructure of Coal Fly Ash Particles, Am. Cer. Soc. Bull., 61, 487-490.

33. Lauf RJ, Rawlston SS (1981) Preparation of Particulates for Transmission Electron Microscopy: An Update, 39th Annual Proc. Electron Microscopy Soc. Amer., Ed. Bailey GW, Claitor's Publishing, Baton Rouge, LA 132-133.

34. Levade C, Couderc JJ, Bras J, Fagot M (1982) Transmission Electron Microscopy Study of Experimentally Deformed Pyrite, Phil. Mag. A, 46, 307-325.

35. Mahajan OM (1985) Determination of Organic Oxygen Content of Coals, Fuel, 64, 973-980.

36. McCartney JT (1970) The Granular Micrinite Component of Coal, Fuel, 49, 409-414.

37. Noro H (1986) Hexagonal Platy Halloysite-Japan, Clay Minerals, 21, 401-415.

38. Raymond Jr R, Gooley R (1978) A Review of Organic Sulfur Analysis in Coal and a New Procedure, SEM 1978;I: 93-107.

39. Raymond Jr R (1982) Electron Probe Microanalysis, A Means of Direct Determination of Organic Sulfur in Coal, ACS Symposium Series #205, 191-203.

40. Reid H, Fuess H (1986) Lamellar Exsolution in Clinopyoxene. Transmission Electron Microscope Observations, Phys. Chem. Minerals, 13, 113-118.

41. Renton JJ (1982) Mineral Matter in Coal, COAL STRUCTURE, Ed. Meyers RA, Academic Press, NY, 283-324.

42. Rouzaud JN, Oberlin A (1985) Raw and Pyrolized Coals: A Preferential Field for Transmission Electron Microscopy, Proc. 1985 International Conference on Coal Science, Pergamon Press, Oxford, New York, Toronto, 657-660.

43. Shuman H, Somlyo AV, Somlyo AP (1976) Quantitative Electron Probe Microanalysis of Biological Thin Specimens: Methods and Validity, Ultramicroscopy, 1, 317-334.

44. Solomon PR, Manzione AV (1977) New Method for Sulfur Concentration in Coal and Char, Fuel, 56, 393-396.

45. Strehlow RA, Harris LA, Yust CS (1978) Submicron-Sized Mineral Components in Vitrinite, Fuel, 57, 185-187.

46. Sudo T, Yotsumoto H (1977) The Formation of Halloysite from Spherulitic Halloysite, Clays and Clay Mineralogy, 25, 155-157.

47. Sudo T, Shimoda S, Yotsumoto H, Aita S (1981) Electron Micrographs of Clay Minerals, Developments in Sedimentology, 31, 104-114.

48. Tseng BH (1986) Direct Measurement of Organic Sulfur Content in Coal Macerals and the Study of Pyrite Decomposition in Coal, (1986). Ph.D. Thesis, University of Illinois at Urbana.

49. Tseng BH, Wert CA, Hausen DM, Hill DL (1987) TEM Analysis of Sulfur and Chlorine in Organic Concentrates from Carbonaceous Gold Ore, Symposium on Process Mineralogy, Denver, February 1987, The Metallurgical Society, In Press.

50. Tseng BH, Buckentin M, Hsieh KC, Wert CA, Dyrkacz GR, (1986) Organic Sulfur in Coal Macerals, Fuel, 65, 385-389.

51. Tseng BH, Ge YP, Hsieh KC, Wert CA (1987) Loss of Organic Sulfur from Coal During Heating, Proc. 2nd International Conference on Processing and Utilization of High Sulfur Coals, Carbondale, Illinois, September 1987, Elsevier.

52. Van Dreysen JC, Doukhan N, Doukhan JC (1985) Transmission Electron Microscope Study of Dislocations in Orthopyroxene $(Mg, Fe)_2Si_2O_6$, Phys. Chem. Minerals, 12, 39-44.

53. Van Krevelen PW (1981) Coal -- Typology, Chemistry, Physics, Constitution, Elsevier, NY, 58-88.

54. Verblen DR, Buseck PR (1981) Hydrous Pyriboles and Sheet Silicates in Pyroxenes and Uralites: Intergrowth Microstructures and Reaction Mechanisms, American Mineralogist, 66, 1107-1134.

55. Wert CA, Hsieh KC (1983) Minerals in Coal - A Transmission Electron Microscope Study, SEM 1983;III: 1123-1136.

56. Wert CA, Hsieh KC, Fraser HL (1986) Chemistry of Coal from Electron Microscopy Measurements, Preprints American Chemical Society Division of Fuel Chemistry, 31, 122-129.

57. Wert CA, Tseng BH, Hsieh KC, Buckentin M, Ge YP (1987) Spatial Variation of Organic Sulfur in Coal, Symposium on Research with Argonne Premium Coal Samples, Amer. Chem. Soc. Fuel Division, New Orleans, August 1987, In Press.

58. Wicks FJ (1986) Lizardite and Its Parent Enstatite: A Study of X-ray Diffraction and Transmission Electron Microscopy, Canadian Mineralogist, 24, 775-778.

59. Winans RE, Crelling JC (Eds.) (1984) Chemistry and Characterization of Coal Macerals, ACS Symposium Series 252, Am. Chem. Soc., Washington, D.C.

Discussion with Reviewers

R. B. Finkelman: Coals are notoriously heterogeneous; ASTM recommends 1000 determinations for petrographic characterization. In view of this heterogeneity, are you confident that 25 analysis of volumes less than 10^{-12} cc can sufficiently characterize the organic-S distribution of a coal.

Authors: Using fine powders of coal, we have found that the average organic sulfur concentration of a specimen can be determined from about 25 measurements. By that time the average has levelled off to an asymtotic value and doubling or quadrupling the number of observations changes that average very little, typically. For a foil of coal prepared for electron microscopy, that sampling of macerals is difficult to achieve. Obtaining the organic sulfur distribution even on fine powders requires many more measurements, also, if information is required about the concentration in the "tails" of the distribution. For such measurements on whole coal or on separated macerals, we commonly take 50 or 100 measurements, but certainly not 1000.

R. R. Martin: Assuming that all the requirements are not to make valid Eq. 1 (thickness of the specimen and absence of fluorescence) what is the order of magnitude one can expect for the limit of detection of organic S in coal by means of EDS?

Authors: That limit is determined by two factors: one's ability to pick out a sulfur Kα line in the background and the accuracy required of the determination. The S-signal can be detected in the background at a level of about 0.05 wt%. The accuracy of measurement of concentration, though, may be ±50%. At organic S concentrations of 0.25 wt%, the S-signal is unmistakable and the accuracy (of a single measurement) may be ±10%, perhaps the accuracy is even higher. Some improvement can be made in signal detection by increasing counting time, since the S-signal commonly goes up faster than the background. But we cannot push the level of detection to 0.01% S, just as users of the SEM and the electron microprobe cannot.